Orion Main Parachute Asymmetry Testing Revisited

Eric S. Ray[1]
National Aeronautics and Space Administration, Johnson Space Center, Houston, TX, 77058

Samuel A. Janssen[2]
Jacobs Technology, Houston, TX, 77058

Limited bridle-level asymmetry data were collected on three Orion main parachute cluster tests early in the development program. The results were published contemporaneously using analysis techniques developed by the Ares parachute program. Both programs seemed to indicate that large parachutes could develop line asymmetries far larger than what was assumed in design guides. Unfortunately, no additional asymmetry data were collected during Orion parachute development to corroborate these results. Recent high-fidelity data from Commercial Crew Program (CCP) parachute system tests reinforce these legacy results. A method was developed to estimate suspension line-level asymmetry by "un-averaging" Orion bridle-level measurements using assumptions gleaned from the recent CCP experience. Efforts were made to improve the visualization of load asymmetry and its relationship with parachute geometric shape deformations.

Nomenclature

CCP	=	Commercial Crew Program
CDT	=	Cluster Development Test (series)
CPAS	=	Capsule Parachute Assembly System
δ_2	=	Suspension line convergence half-angle (from centerline)
D_o	=	Nominal parachute diameter based on reference area, $D_o = \sqrt{4 \cdot S_o / \pi}$
D_p	=	Projected diameter
EDU	=	Engineering Development Unit (test series)
F_{bridle}	=	Measured tension force in a parachute dispersion bridle
F_{riser}	=	Measured tension force in a parachute riser
F_{sl}	=	Estimated tension force for individual parachute suspension line
GPS	=	Global Positioning System
IMU	=	Inertial Measurement Unit
L_S	=	Suspension line length
MDT	=	Main Development Test (series)
MLLR	=	Main (Suspension) Line Length Ratio test (aka CDT-2-1)
MPCV	=	Multi-Purpose Crew Vehicle (Orion)
RC	=	Ramp Clear (usually chosen as start of test)
s	=	Asymmetric suspension line load distribution factor
SAR	=	System Acceptance Review
S/N	=	Serial Number
S_o	=	Parachute canopy full open reference area based on constructed shape including vents and slots
SPAN	=	Synchronized Position Attitude & Navigation
TMS	=	Tension Measuring System

[1] Analysis Engineer, Aeroscience Branch, NASA Johnson Space Center/EG3, AIAA Senior Member.
[2] Analysis Engineer, Aerosciences and Flight Mechanics, 2224 Bay Area Blvd, Houston TX, non-member.

I. Introduction

FOR a brief window in its design cycle, the main parachutes of the Orion/Multi-Purpose Crew Vehicle (MPCV) had a design which facilitated partial measurements of line asymmetry. The Capsule Parachute Assembly System (CPAS) completed formal System Acceptance Review (SAR) in September of 2019. Nearly a decade earlier, candidate variants of the 116 ft D_o quarter spherical ringsail main parachutes underwent testing at the US Army Yuma Proving Ground (YPG). These intermediate designs collected eight groups of ten suspension lines into bridles, which then came together in a confluence to attach to the riser. These bridles were non-invasively instrumented for loads. The later CPAS main parachute design transitioned to continuous suspension lines, bundled together to form the riser, which did not offer any breaks for in-line loads instrumentation nor any intermediate grouping for a moderate number of passive instruments.

The data collected on these three CPAS flight tests were described in Ref. 1 using analysis methods developed by Marshall Spaceflight Center (MSFC) for the Ares program.[2] Guidance from the Knacke Parachute Recovery Systems Design Manual[3] recommends an asymmetric loading factor (s) of 1.1. However, CPAS published bridle-level asymmetric loading on the order of 1.5 and as high as 1.9 for the worst case. With little validation data, the CPAS results were only tentatively accepted. Modern high-quality main parachute asymmetry test data collected for the Commercial Crew Program (CCP) corroborate many of the earlier CPAS findings.

The three tests under consideration used flat platforms suspended under a confluence fitting. The load instrumentation is shown in Figure 1. Individual parachute riser loads were measured with in-line strain links rated to 30K lbf. Each parachute had eight Tension Measuring System (TMS) II units installed on dispersion bridles. These second generation TMS units measured the bridle tension as a compressive force against a strain plate. The units were too large to measure individual suspension lines.

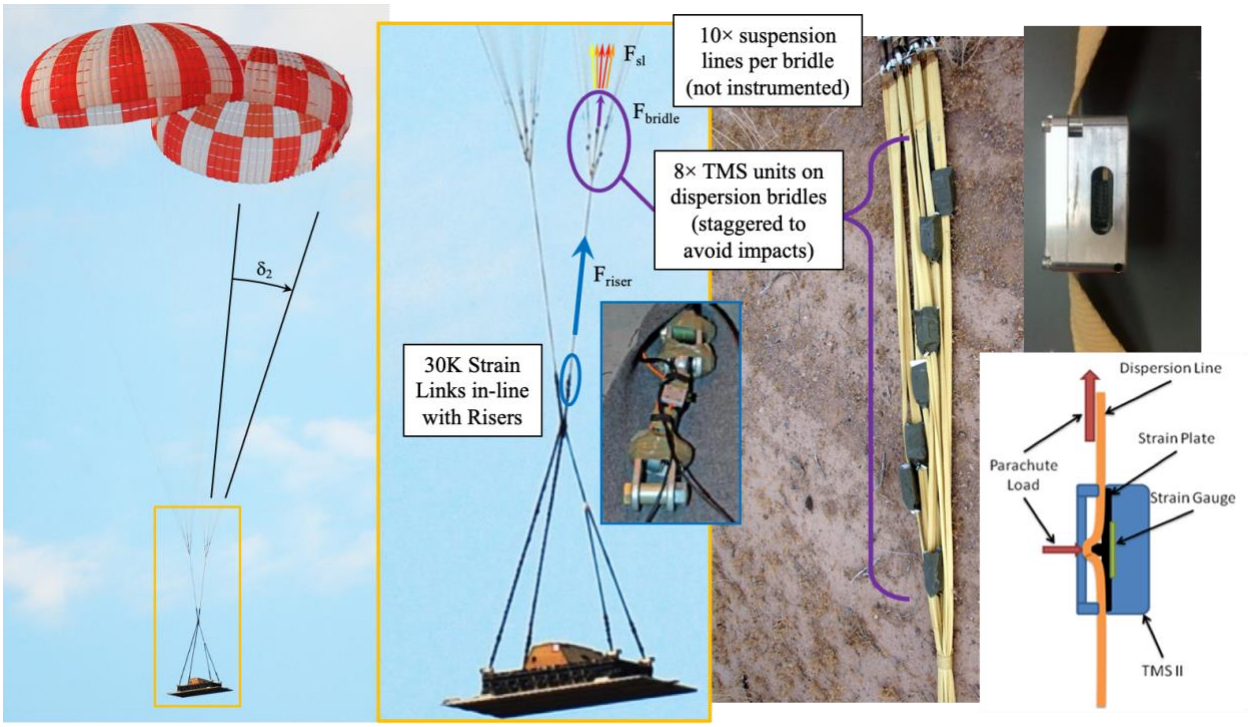

Figure 1. Riser and bridle loads instrumentation on CPAS Gen II cluster platform tests.

In addition to maturing parachute design, the second series (Gen II)[4] of CPAS flight testing was an opportunity to develop test techniques, evaluate measurement devices, and improve imagery in preparation for Engineering Development Unit (EDU)[5] testing. Gen II tests used the high-quality Global Positioning System (GPS)/Inertial Measurement Unit (IMU) hardware to prevent signal dropout during extraction, and improve velocity and position readings.[6,7] High Definition (HD) cameras with solid state recorders were installed on the payload. However, the camera models used on these tests would sometimes lose focus with sudden jarring, and were later replaced with more stable cameras with higher resolution. High Speed (HS) cameras[8] were used on EDU tests but were likewise not available for Gen II testing. While still photos were taken from the ground and an orbiting helicopter for these tests,

memory cards limited the number of images captured to a small fraction of what was recorded on later tests. Nevertheless, it is possible to draw some conclusions from this information.

A sample plot of previously published CPAS asymmetry at the peak first stage load for Cluster Development Test (CDT)-2-1 is shown in Figure 2. Asymmetry was computed as a percentage above and below each canopy mean at the time of each peak load. Displaying the data as points on an octagon is less than ideal because each point actually represents a distributed load along a section of the canopy. Further, it is somewhat difficult to identify the points relative to the 0% datum. It would be better to use other visual cues, such as color gradients, to highlight areas of extreme loading. Video shows that the skirts were elongated and parallel, presumably with the highest asymmetries on the semi-major axes. However, the roll angle of the canopies is random such that the numbering of the dispersion bridles happen to appear perpendicular to each other in the polar plot.

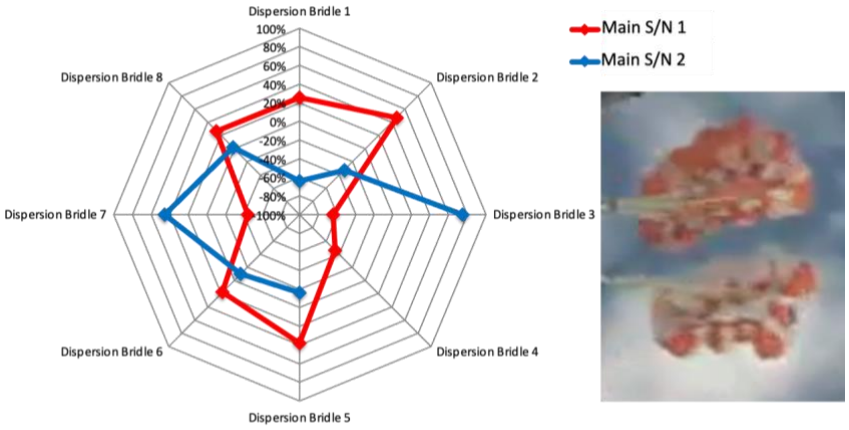

Figure 2. Legacy polar plot depicting CDT-2-1 first stage peak load asymmetry. The parachute skirts are parallel, but the bridle numbering makes them appear perpendicular.

The purpose of this analysis is to improve the visualization of asymmetry by combining loads data with physical geometry in an intuitive manner. Given some assumptions about load variation, it is even possible to estimate asymmetry at the suspension line level.

II. Analysis and Visualization Methodology

Parachute asymmetry can be measured at several levels depending on the methods of instrumentation. Individual riser loads indicate cluster load share, usually caused by lead-lag behavior.[9] Localized shape changes mean that asymmetry at the bridle level (Eq. 1) will be of lower magnitude than the potential asymmetry at the suspension line level (Eq. 2). Knowing that all instrumentation will have measurement errors, it is good practice to compare the sum of component level readings with direct readings at a higher level. For example, the sum of risers is always compared to the cluster load from IMU accelerometers.[10] In the same way, the sum of bridle loads are compared with individual riser loads. For consistency, CPAS convention is to compute asymmetry factor relative to the average of all component readings rather than the normalized riser reading. This avoids the need to account for the suspension line geometric convergence half-angle (δ_2).

$$\text{Bridle Asymmetry Factor} = \frac{F_{bridle}}{\frac{1}{8}\sum_{i=1}^{i=8}(F_{bridle})_i} \text{ or } \frac{F_{bridle}}{\left(\frac{F_{riser}}{8\cdot\cos(\delta_2)}\right)} \tag{1}$$

$$\text{Suspension Line Asymmetry Factor} = \frac{F_{sl}}{\frac{1}{80}\sum_{j=1}^{j=80}(F_{sl})_j} \text{ or } \frac{F_{sl}}{\left(\frac{F_{riser}}{80\cdot\cos(\delta_2)}\right)} \tag{2}$$

A close examination of the previously published CPAS TMS data uncovered some deficiencies. Each unit has its own internal timing not connected to an absolute channel. To properly compute asymmetry, all the data must be synchronized to each other based on common signal, such as the initial load ramp-up. The previous analysis assumed all TMS units were activated simultaneously, though each unit had separate pin pulls. TMS data with common relative timing were then synchronized to the riser loads based on riser load ramp-up, which has an absolute time channel provided by the payload avionics. The TMS units were initially assumed to have a constant recording rate of 1000 Hz. However, the unloading traces at touchdown tended to occur significantly after the measured riser unloading, meaning that the actual rate for each unit was a somewhat faster unique value (such as dt = 0.0009717 s for TMS S/N 18). Most TMS units also had a non-zero initial signal, indicating a slight bias on the order of 100 lbf. These average biases were subtracted out (tared). An example of corrected TMS loads from CDT-2-1 Main S/N 2 is shown in Figure 3. In many

cases, at least some of the TMS units failed to record data. Missing data had to be approximated by either averaging data on adjacent bridles, or by mirroring data when bilateral symmetry was observed.

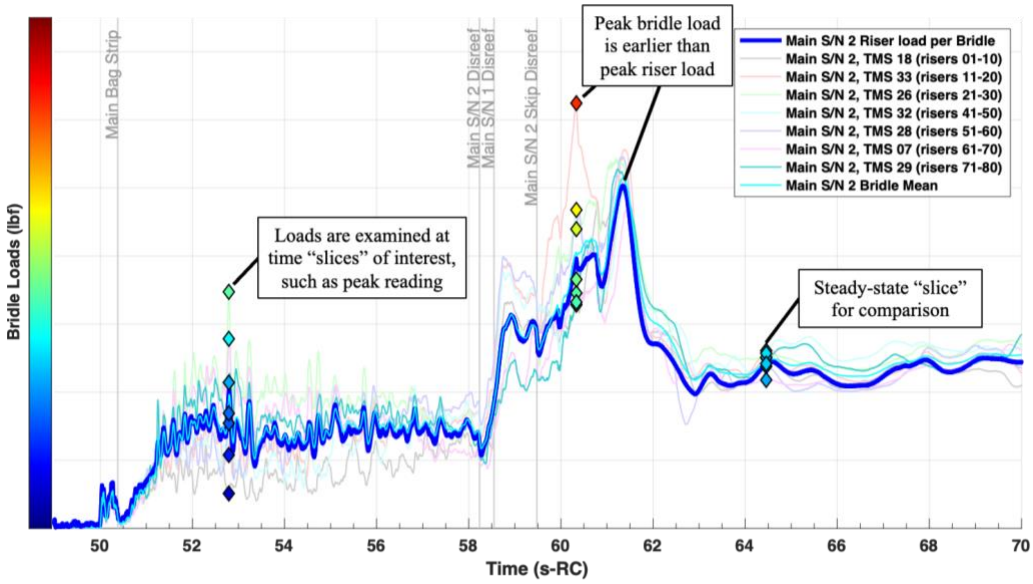

Figure 3. Sample corrected TMS readings compared to normalized riser load. Note that one of the eight TMS units did not collect data and an assumed reading was necessary to compute statistics.

The normalized riser strain link (blue) compares favorably with the bridle average (cyan) during inflation. After inflation, the magnitude of the bridle mean slightly exceeds the normalized riser as expected, because cosine effects have not yet been corrected. The 3-D geometry of the canopy can be determined by combining upward-looking imagery from payload cameras with side views from chase aircraft.[11] However, analysis has shown that cosine effects between a riser and suspension lines are negligible for most of inflation and only cause errors up to 3% after full open.

Test results for each bridle were examined at events of interest as indicated by colored diamonds corresponding to the figure color bar. These indicate the peak bridle load in first and second stages, as well as a post-inflation time for comparison. Note that the peak second stage bridle load occurs nearly one second before the peak riser load. Component level peaks are often not concurrent with higher-level peaks. It will be shown that loads at distinct events are more useful than global peak asymmetry factors from an engineering perspective.

A relatively simple interpolation method was developed to estimate individual suspension line loads based on the bridle loads. Figure 4 shows a diagram illustrating the "un-averaging" method and the results for all eighty suspension lines on Main S/N 2 from CDT-2-1 at the time of peak second stage load. A trivial approximation would be to assume all ten suspension lines take an equal share of their corresponding bridle with discontinuities to adjacent bridles, as illustrated by the filled diamonds. However, it would be better to assume a gradual transition from line to line and from bridle to bridle. All the suspension line groups should still sum up to the corresponding bridle measurement, which are conveyed as areas. This area equivalence can be enforced by approximating groups of suspension line forces as adjoining parallelograms with a common peak. Boundaries are defined by the averages of adjacent bridles. More sophisticated interpolation methods using smoothing and relaxation algorithms may be attempted in the future. However, the current method produces plausible results when compared with recent individual suspension line flight test data.

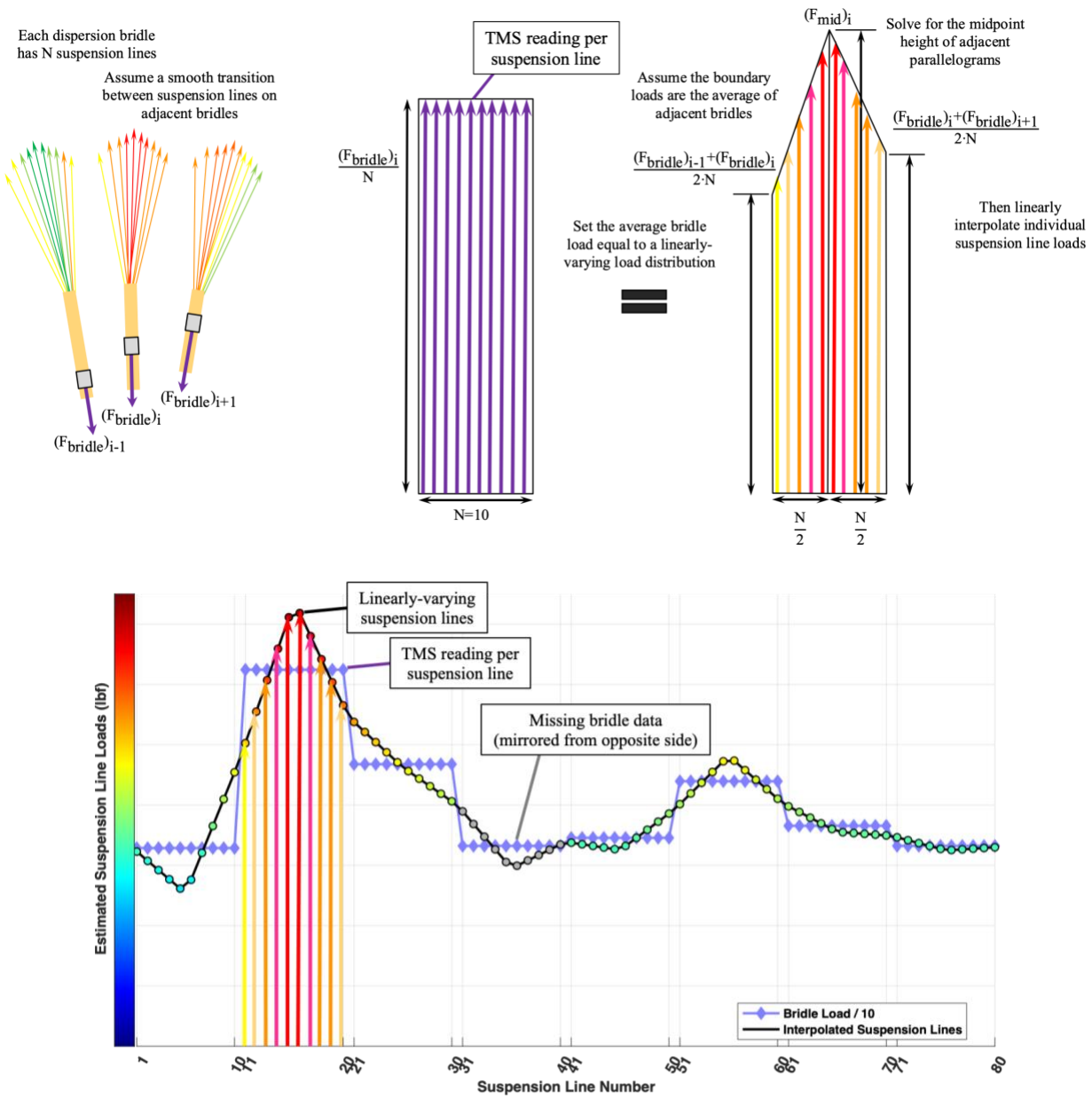

Figure 4. Sample estimated suspension line readings using linear interpolation. The sum of groups of ten suspension lines are forced to sum up to the corresponding measured bridle reading.

Individual suspension line data are useful when applied to flight test imagery. This provides insight into the physical relationships between inflating shapes and localized stress concentrations. The following sections show analysis of the three CPAS Gen II tests under consideration. The relationship between asymmetric loading and canopy distortion at the crown and skirt are investigated in a companion paper.[12]

III. CDT-2-1 Modified Line Length Ratio (MLLR) Test with Inadvertent Skipped Second Stage

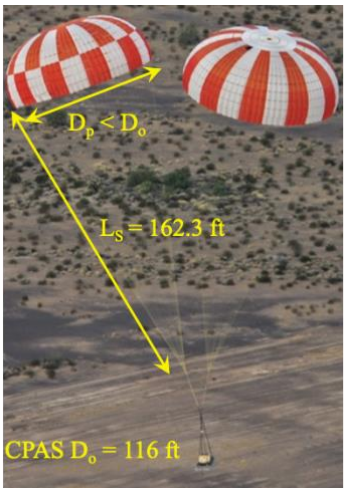

Figure 5. CDT-2-1 Modified Line Length Ratio Configuration.

CDT-2-1 was a two-main test intended to evaluate a larger suspension line length ratio, L_S/D_o: the length of the suspension lines (L_S) divided by the reference diameter of the parachute (D_o). The test modified the previous CPAS length ratio of 1.15 to the longer 1.44 ratio used by Apollo. The CDT-2-1 lines are shown in Figure 5. The longer ratio was later incorporated into the EDU design. During inflation, a load share discrepancy was quickly apparent on CDT-2-1 with Main S/N 2 (orange crown) appearing physically larger than Main S/N 1 (white crown). The additional load caused a failure in the second stage reefing system on Main S/N 2, where it skipped second stage directly to full open. The reefing system was later reinforced and did not fail in subsequent tests.

The TMS bridle loads for both canopies are plotted Figure 6 with diamonds to mark bridle loads at times of interest for each. The skipped second stage caused a long delay before the lagging canopy finally inflated to full open. A time history of the computed bridle-level asymmetry factors is shown in Figure 7. Main S/N 1 (pink) has the highest asymmetry factors while its actual load is very low. Obviously, asymmetry factor should therefore not be a valid performance metric at such times.

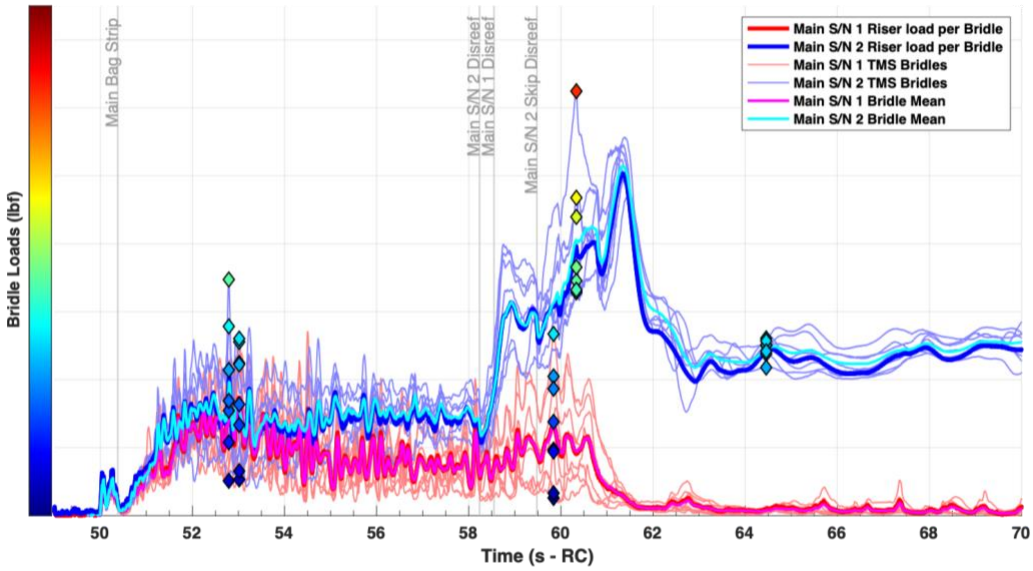

Figure 6. CDT-2-1 TMS bridle load histories. Individual inflation stage peak TMS readings and a steady-state reading are marked with diamonds.

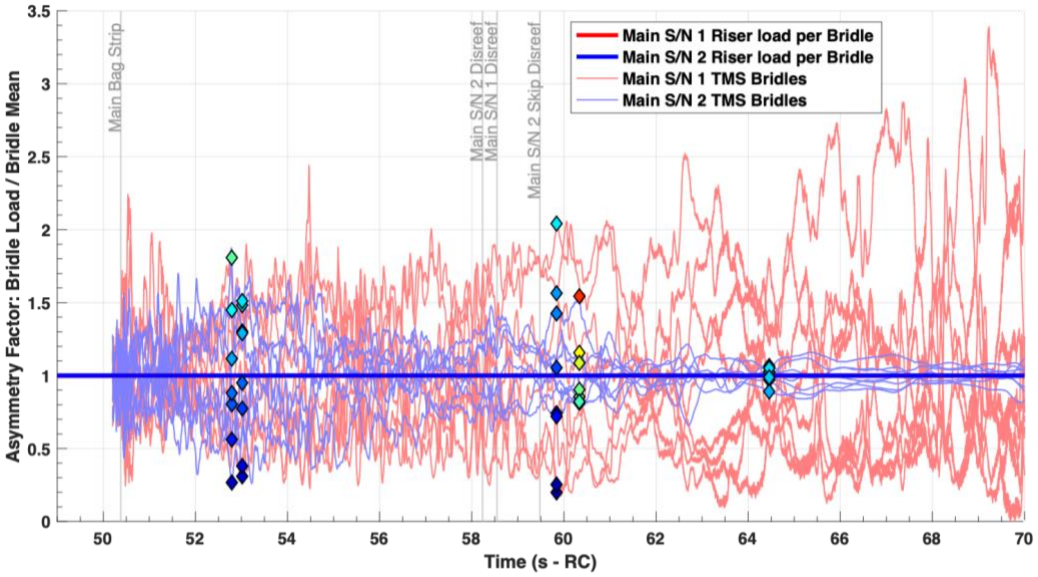

Figure 7. CDT-2-1 bridle-level asymmetry time history. Individual data at the same peak load instants are indicated with diamonds, showing little correlation between asymmetry and loads.

A more meaningful way to plot asymmetry factor is as an independent variable with load as the dependent variable, as in Figure 8. This formulation shows that higher loads are generally associated with lower asymmetry and vice-versa. The peak load (red diamond) for Main S/N 2 at the skipped second stage has an asymmetry factor of over 1.5, while negligibly low loads on Main S/N 1 have asymmetry factors up to 3.4. The former is a useful design point while the latter is of no practical concern.

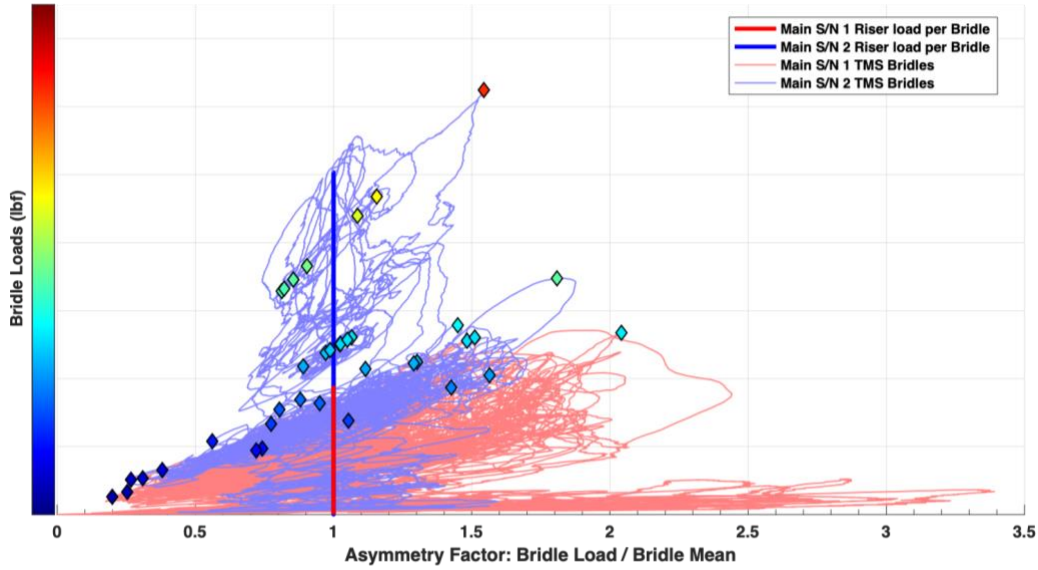

Figure 8. CDT-2-1 bridle loads vs. asymmetry factor. The bridle asymmetry associated with the peak skipped stage load is over 1.5, while instants of lower loads have higher asymmetry.

The time histories of individual suspension lines for both canopies were estimated using the previously described linear interpolation and are plotted in Figure 9. The peak suspension line load is further from the suspension line average than the peak bridle load is from the bridle average, indicating that higher asymmetry at the finer level.

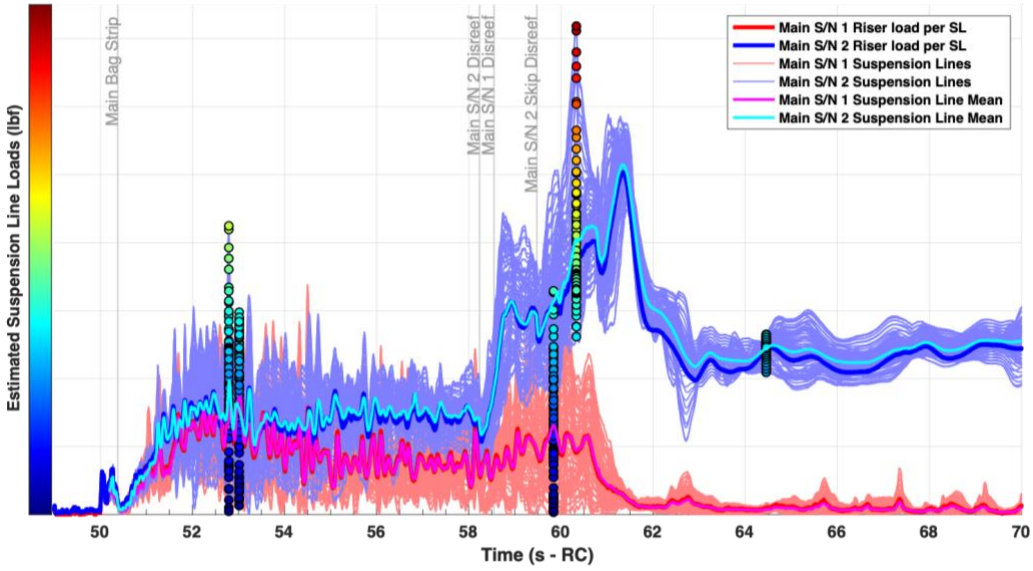

Figure 9. CDT-2-1 estimated individual suspension line loads.

Figure 10 shows the suspension line-level asymmetry factor and corresponding loads. At this level, the asymmetry associated with the skipped stage event has increased to nearly 1.8.

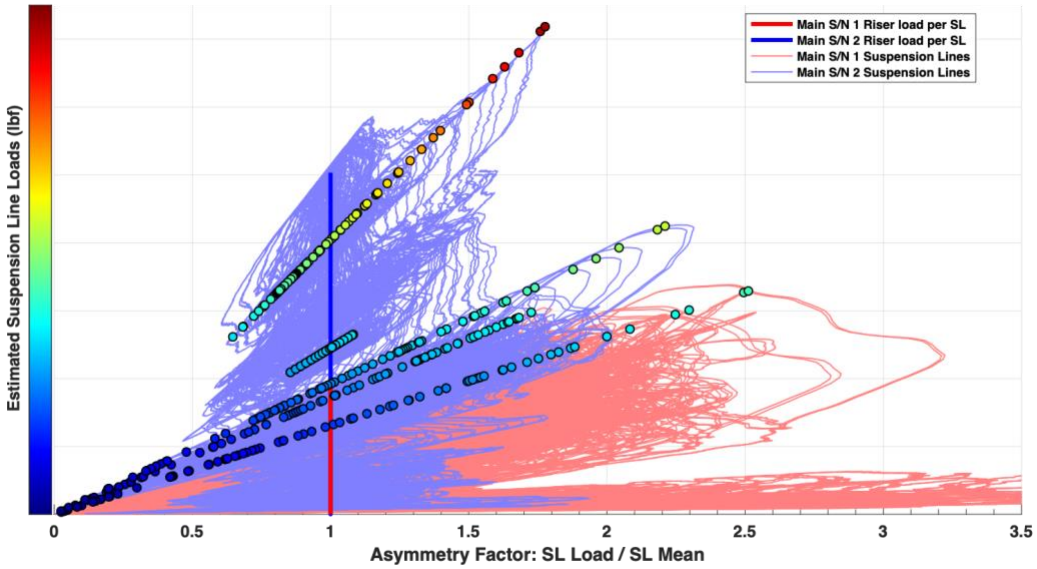

Figure 10. CDT-2-1 estimated suspension line loads vs. asymmetry factor. The suspension line asymmetry associated with the peak skipped stage load is about 1.8.

The shapes of the canopies develop based on a complex fluid-structure interaction including the mutual aerodynamic interference between canopies. Clusters of two main parachutes tend to elongate as ellipses at the skirt with circumferences defined by reefing line lengths.[13] In turn, a relationship exists between the suspension line asymmetry at the skirt and the pressurization at the crown. To investigate this, a method was developed to combine a gross characterization of canopy shape with line load data. Time-synchronized images from multiple perspectives were examined at the times of interest to subjectively determine which panels were unpressurized (marked with a 0) and which were fully pressurized (marked with a 1 or blank). This would have been impossible without the two-tone color patterns and the black ink markings on gores 79-80. Later CPAS and CCP tests added even more useful canopy markings. The pressurization maps for both mains on this test are shown in Figure 11.

Main S/N 1 Pressurization at Peak First Stage

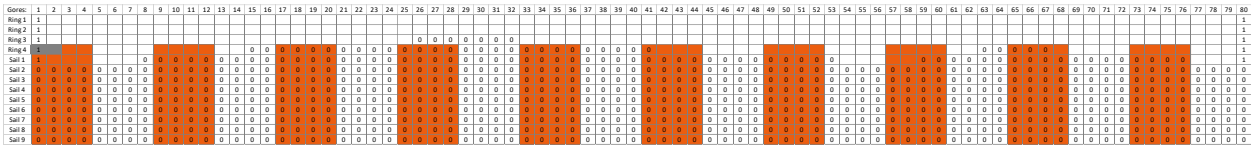

Main S/N 1 Pressurization at Peak Second Stage

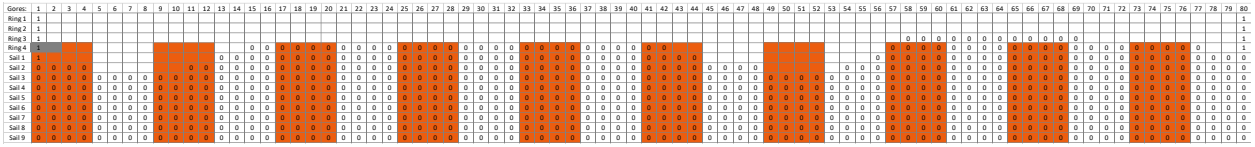

Main S/N 2 Pressurization at Peak First Stage

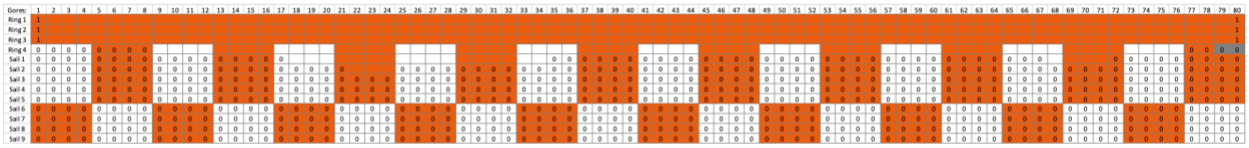

Main S/N 2 Pressurization at Peak Skipped Stage

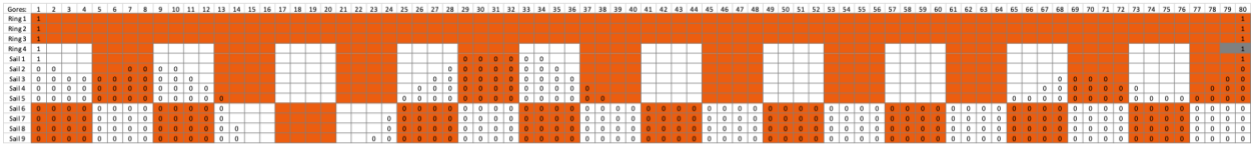

Main S/N 2 Pressurization After Inflation

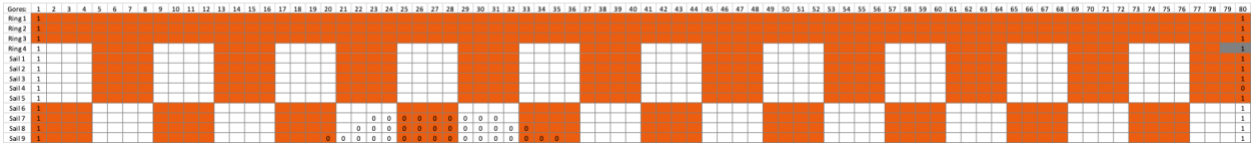

Figure 11. CDT-2-1 Main S/N 1 and 2 pressurization maps. 0 = unpressurized, 1 (or blank) = pressurized.

To visualize the load distributions on the parachutes, features had to be identified on images. This was performed using MATLAB by reading in frames corresponding to time slices. 2-D coordinates were then manually selected for bridle convergence points and intersections of suspension lines with the skirt. Accuracy was limited by the available imagery resolution. The selected coordinates were saved to data files. This information could then be superimposed on images as line segments to depict suspension lines and dots to depict interface points on skirt. The colors of these features were automatically adjusted according to suspension line load magnitude scaling. Because the identification of features is more difficult for tightly reefed stages, a useful technique is to work chronologically backward from full open so easily identified features can be traced to earlier frames.

Images captured closest to the first and second stage peak loading events are augmented with colored estimated suspension line load distributions in Figure 12 and Figure 13, respectively. Ground-to-air still photos are shown on the left. Upward-looking payload video frames corresponding to each peak load time are shown in the center with boundary suspension lines labeled. The polar plots to the right are rotated to align with the upward-looking video frames to confirm that the elongated geometric shapes tend to align with the regions of higher load. The normalized peak riser loads for each canopy are depicted as red or blue circles. Therefore, areas outside each circle have higher than average loading and areas inside each circle are relatively unloaded. Pressurized panels are represented on the polar plots as sectors to indicate that areas of higher crown pressurization tend to be related to areas of higher suspension line loads at the skirt. The background panels are colored according to their corresponding physical markings on each canopy. The color bars use a common scale to allow for easy comparison of loads between canopies. Inferred data from the missing bridle on S/N 2 are highlighted in gray. The polar plot for first stage of Main S/N 1 makes a “butterfly” shape, which is common for clusters of two parachutes. The load share discrepancy and shape distortions caused more pointed shapes toward one end of each canopy. Each “arrow” tends to point toward regions where more panels are pressurized at each crown.

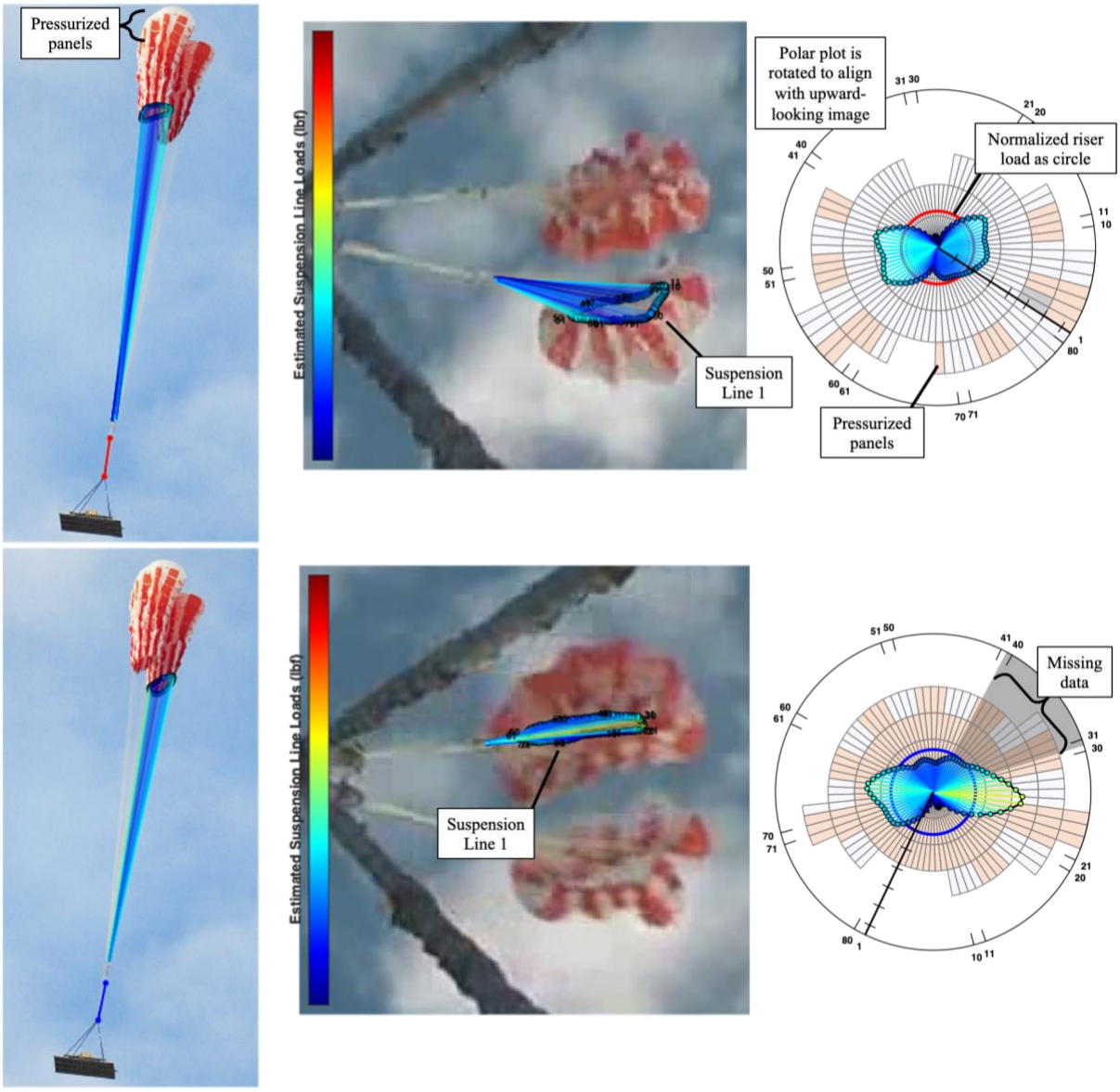

Figure 12. CDT-2-1 first stage estimated peak load distributions for Main S/N 1 (top) and Main S/N 2 (bottom).

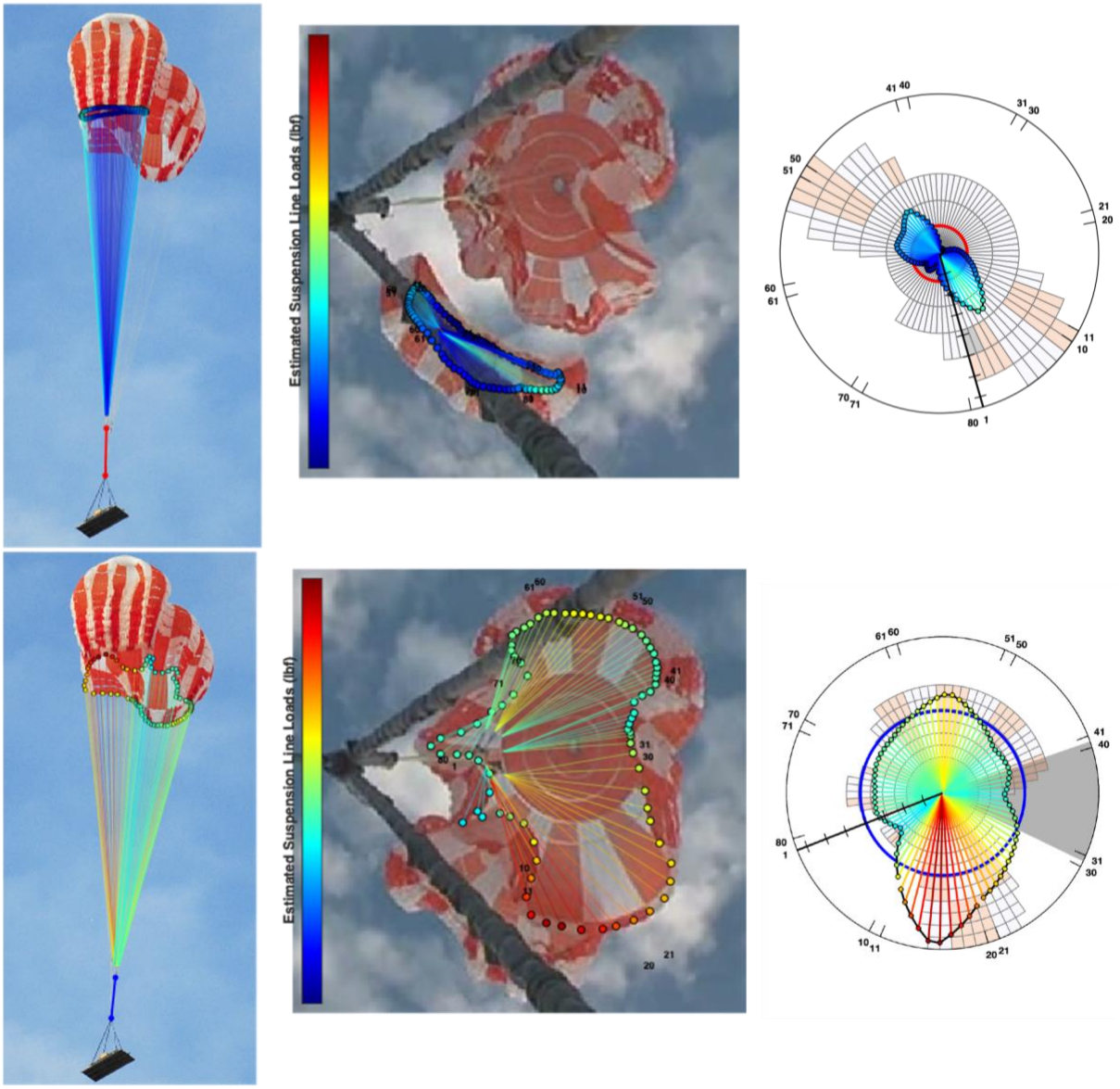

Figure 13. CDT-2-1 second stage estimated peak load distributions for Main S/N 1 (top) and skipping Main S/N 2 (bottom).

After the skipped second stage, Main S/N 2 achieves a very low asymmetry full open state as depicted in Figure 14. The physical shape is nearly circular, corresponding to the circular polar plot.

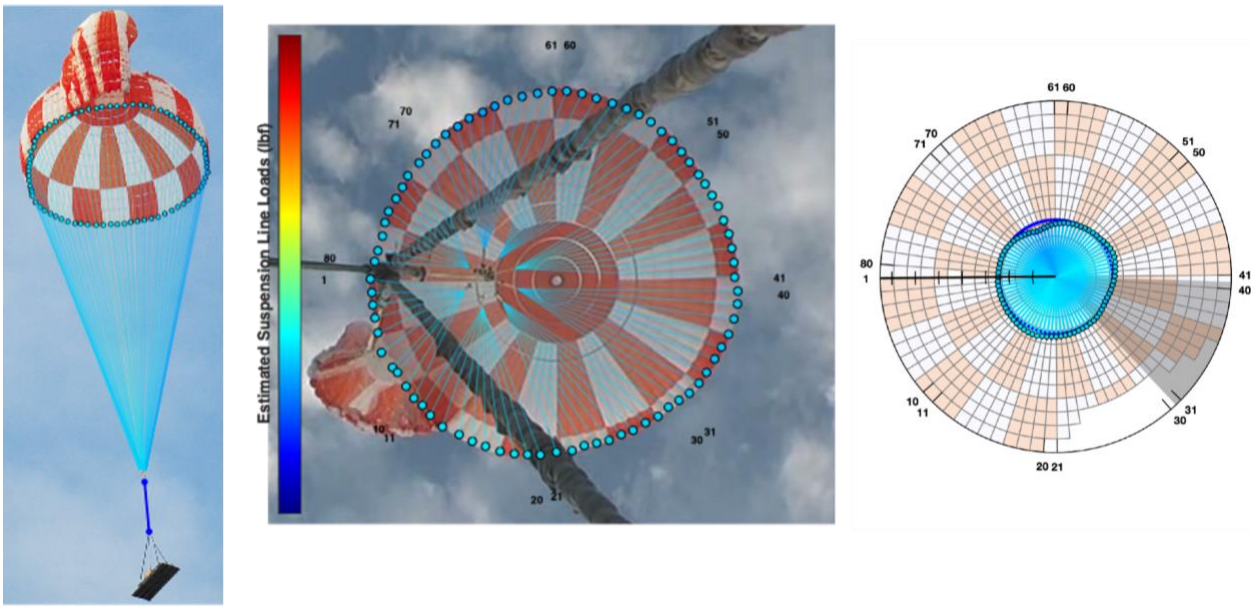

Figure 14. CDT-2-1 fully inflated estimated load distribution for skipping Main S/N 2.

IV. CDT-2-2 Modified Porosity Two-Main Test with Uniform Cluster Inflation

Figure 15. CDT-2-2 modified porosity.

CDT-2-2 tested a cluster of two mains with an intermediate design. This test and CDT-2-3 intended to improve cluster stability by increasing the geometric porosity with a larger ring gap and "window" panels, as shown in Figure 15. However, the suspension lines were the shorter original length. The EDU design would later incorporate both the modified porosity and the longer lines. This test had among the most equal inflation between canopies of any CPAS or CCP test so far.

Time histories of the measured bridle loads and interpolated suspension line loads are shown in Figure 16 and Figure 17, respectively. Main S/N 4 did not collect data on two bridles. Main S/N 5 did not collect data on bridle 5. The missing data caused some discrepancies between the normalized riser load and average line loads. The times of disreef and peak loads are almost simultaneous between canopies. Because this was a less stressing case than CDT-2-1, the color bar scale was lowered to better highlight the overall range.

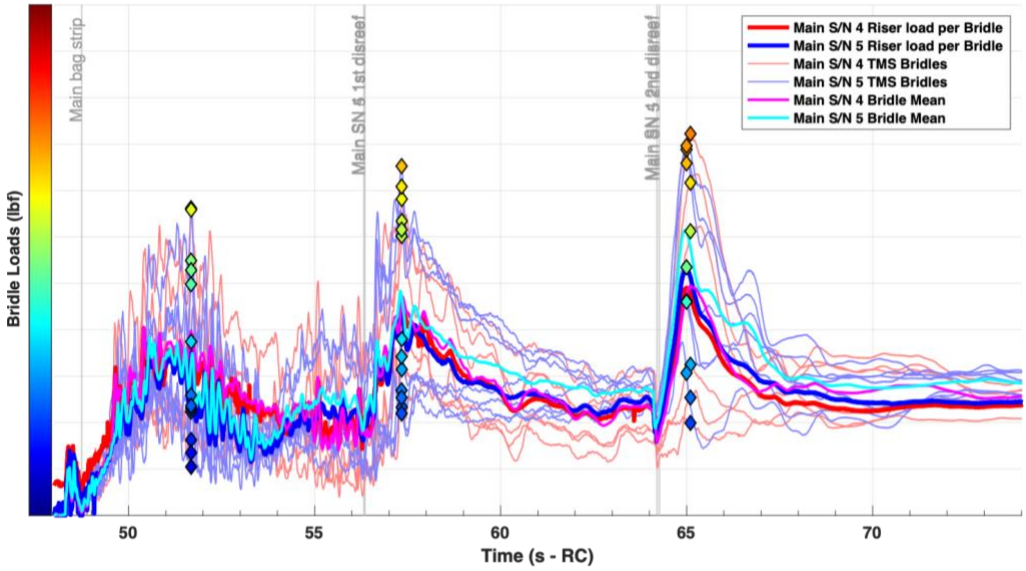

Figure 16. CDT-2-2 TMS bridle load histories.

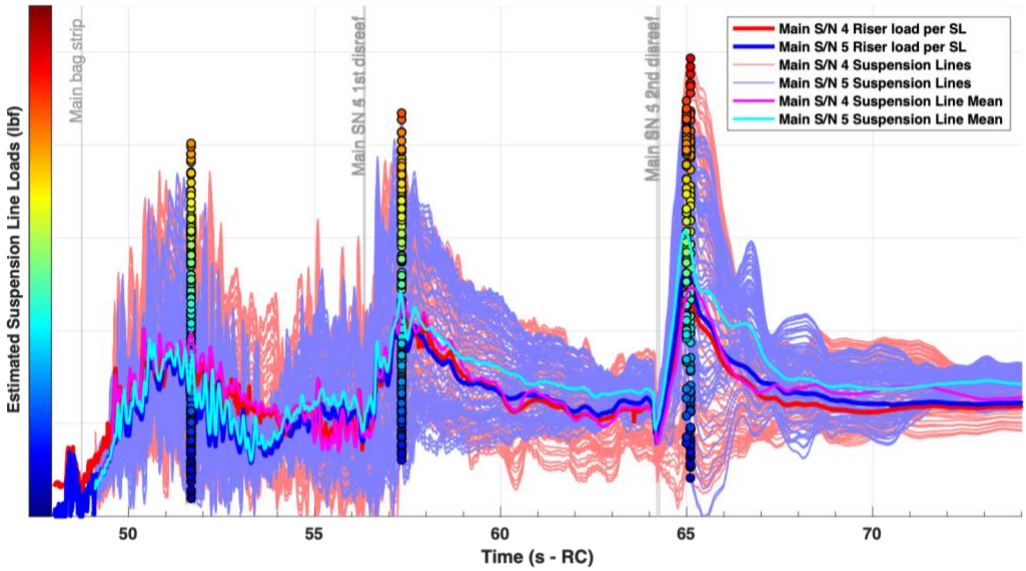

Figure 17. CDT-2-2 estimated suspension line load histories.

The bridle loads are plotted with asymmetry factor as the independent variable in Figure 18. The highest peak load has an asymmetry factor of about 1.7 on Main S/N 4. As indicated in Figure 19, the estimated suspension line-level asymmetry factor is slightly over 2 when the parachutes observe peak loads at the full open.

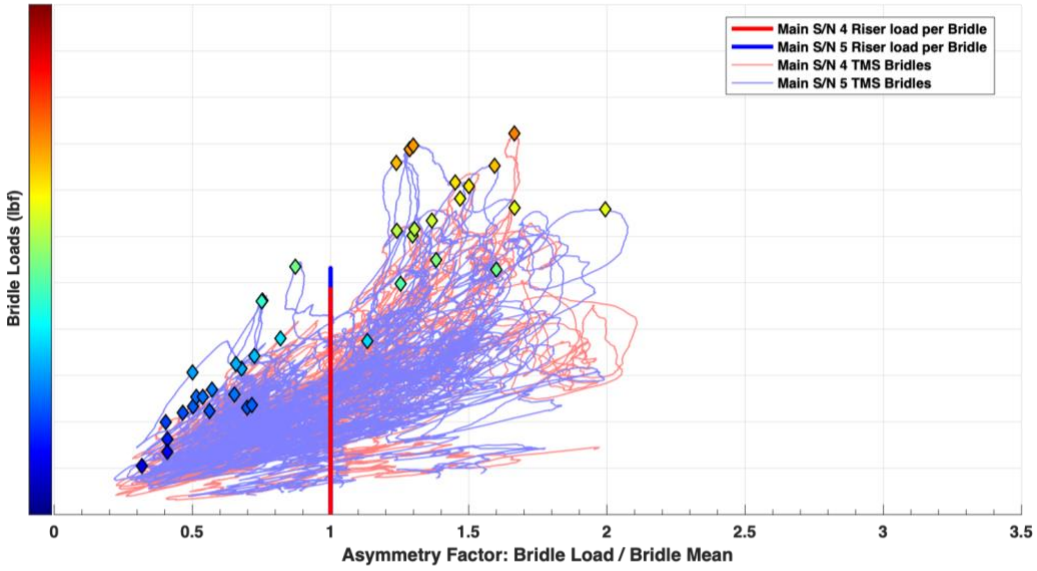

Figure 18. CDT-2-2 bridle load vs asymmetry factor. The peak load has an asymmetry factor of about 1.7.

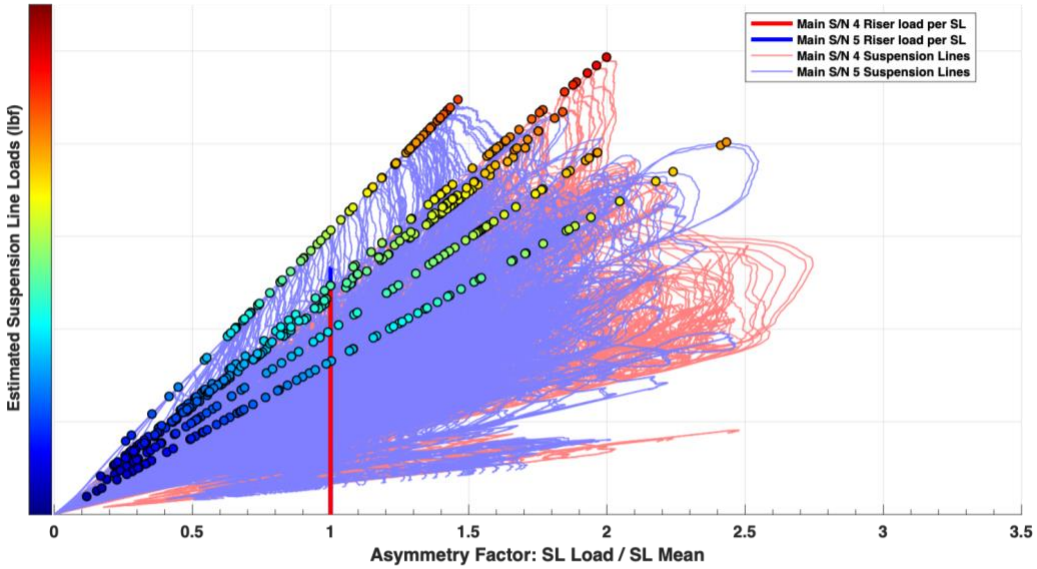

Figure 19. CDT-2-2 estimated suspension line load vs asymmetry factor. At the finer resolution, the peak load has an asymmetry factor of about 2.1.

Augmented imagery and polar plots for the peak first stage loads are shown in Figure 20. There was some confusion with the locations of the TMS units on S/N 4, so some assumptions were made such that the readings align with the physical shapes. The similar inflated shapes between canopies lead to similar "butterfly" polar plots. This trend holds true for peak second stage loads (Figure 21) and peak full open loads (Figure 22).

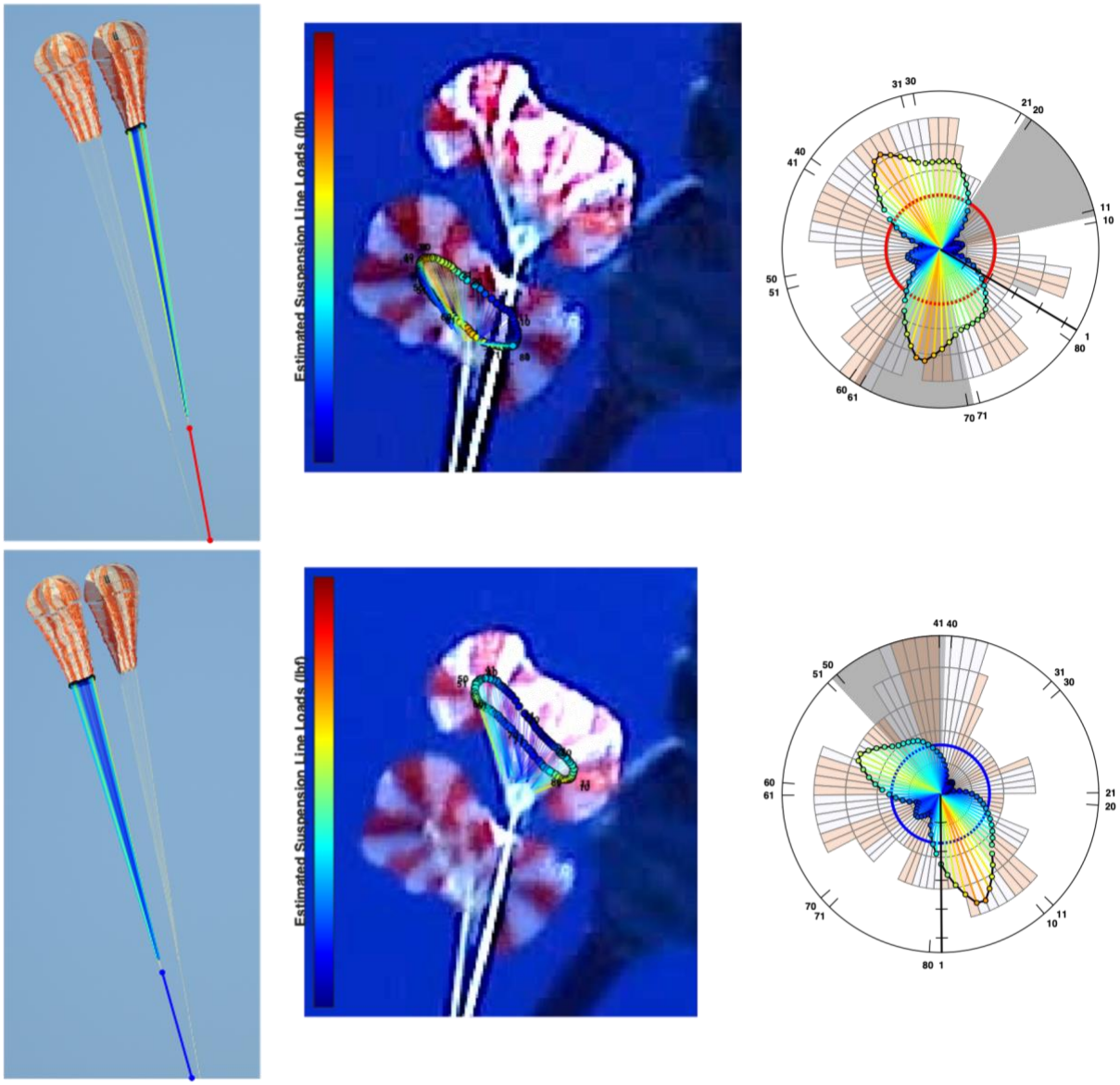

Figure 20. CDT-2-2 first stage estimated peak load distributions for Main S/N 4 (top) and Main S/N 5 (bottom).

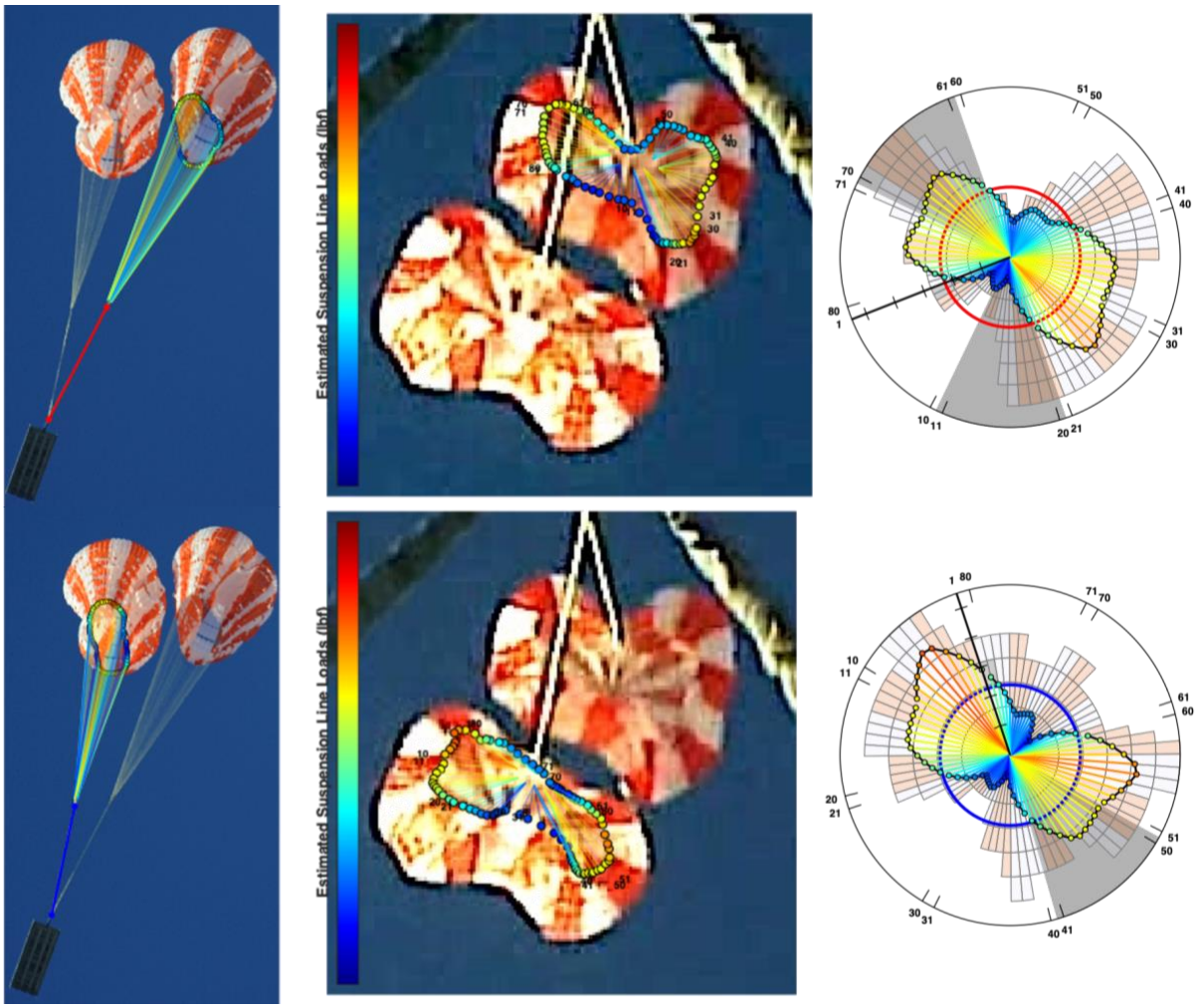

Figure 21. CDT-2-2 second stage estimated peak load distributions for Main S/N 4 (top) and Main S/N 5 (bottom).

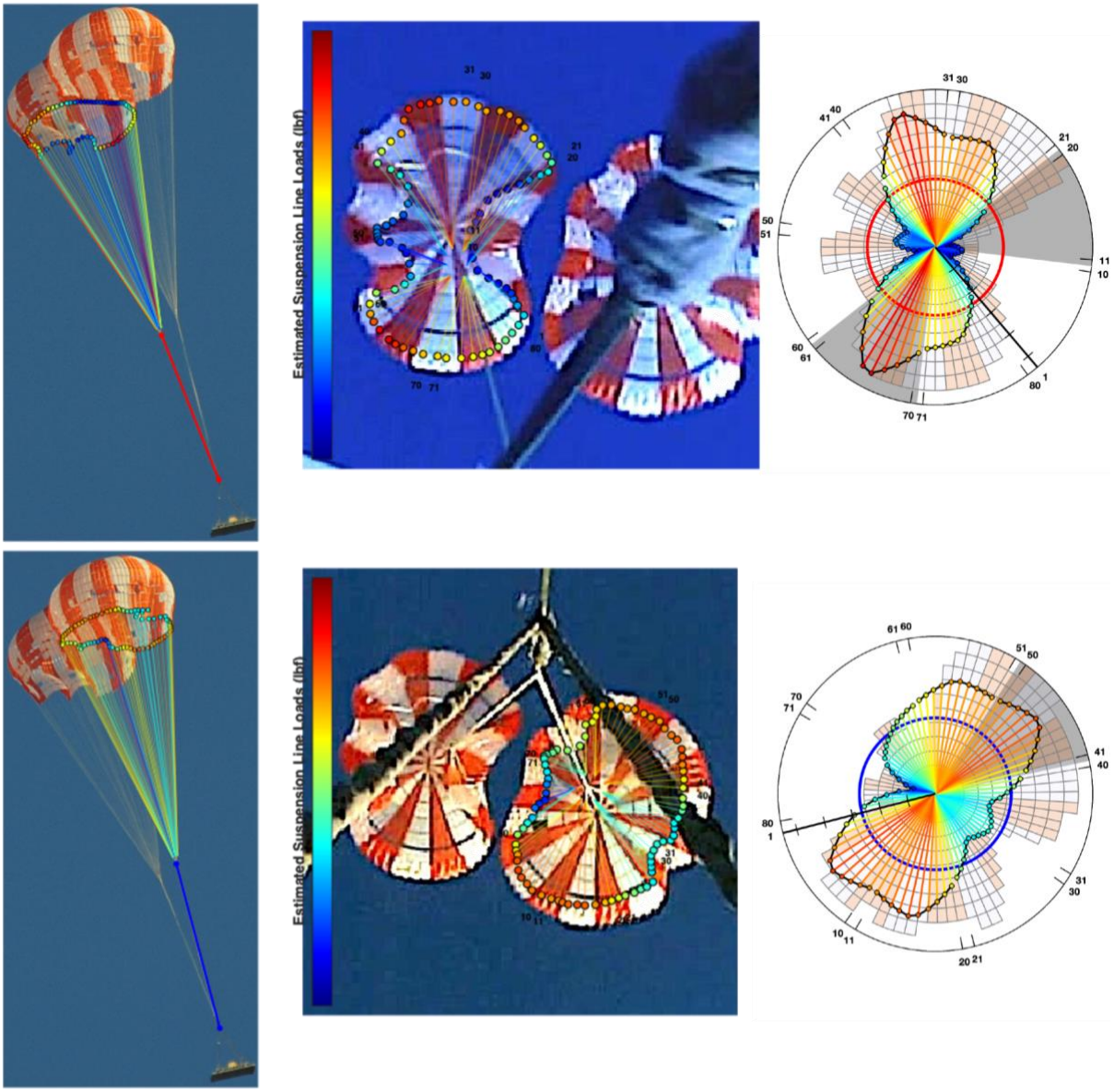

Figure 22. CDT-2-2 full open estimated peak load distributions for Main S/N 4 (top) and Main S/N 5 (bottom).

V. CDT-2-3 Modified Porosity Three-Main Test

Having successfully tested the added porosity design with a single main (MDT-2-3) and two mains (CDT-2-2), CPAS next tested the nominal configuration of three mains. The CDT-2-3 configuration is shown in Figure 23. Due to the limited number of TMS units, only two of the three canopies were instrumented for asymmetry.

Because the inflations were shared by three canopies, the absolute measured loads were lower on CDT-2-3 than on CDT-2-2 (using the same color bar scale). The measured bridle loads on S/N 3 and S/N 4 compare favorably with normalized strain link riser loads in Figure 24. All eight TMS units collected data on Main S/N 3 (red), but one unit failed on Main S/N 4 (blue) and is interpolated with adjacent bridles. This allows for good agreement between the normalized riser loads and average line loads. The times of peak TMS loads (marked with diamonds) tend to spread out between canopies and from corresponding riser peaks, probably due to the irregular shapes induced from cluster interference. Main S/N 5 (green) was the first canopy to disreef to full open and took the greatest load share.

Figure 23. CDT-2-3 Configuration.

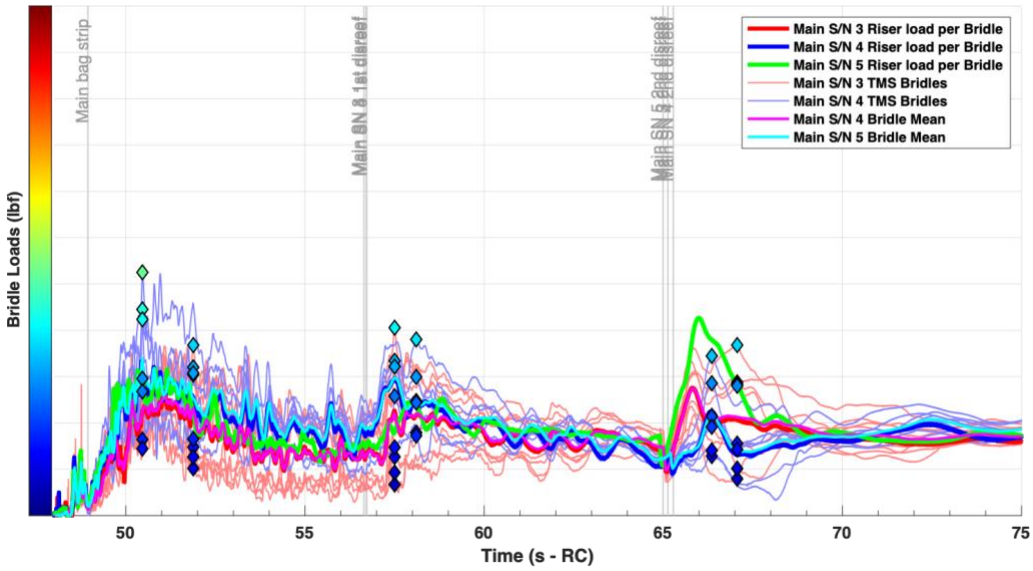

Figure 24. CDT-2-3 measured bridle load histories for two of three canopies.

Suspension line loads were estimated for the two instrumented canopies in Figure 25. Unfortunately, it is not possible to estimate the asymmetry loads on Main S/N 5 due to the lack of instrumentation. Its higher riser load would imply that it experienced the highest component loads.

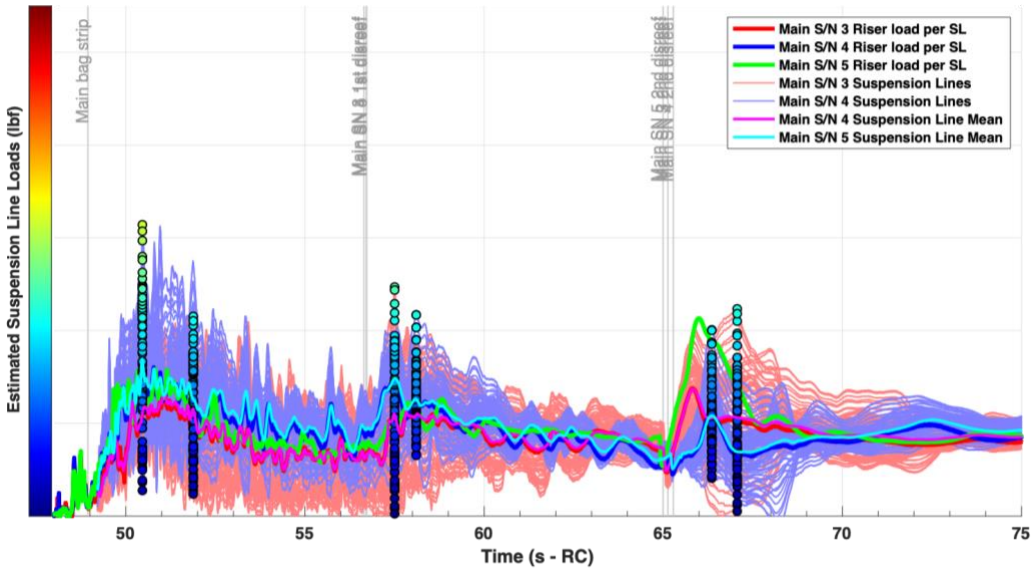

Figure 25. CDT-2-3 estimated suspension line load histories for two of three canopies.

Asymmetry factors are shown at the bridle level and suspension line level in figures Figure 26 and Figure 27, respectively. The asymmetry factor at the peak load increases from about 1.5 to about 2.0 at the higher resolution.

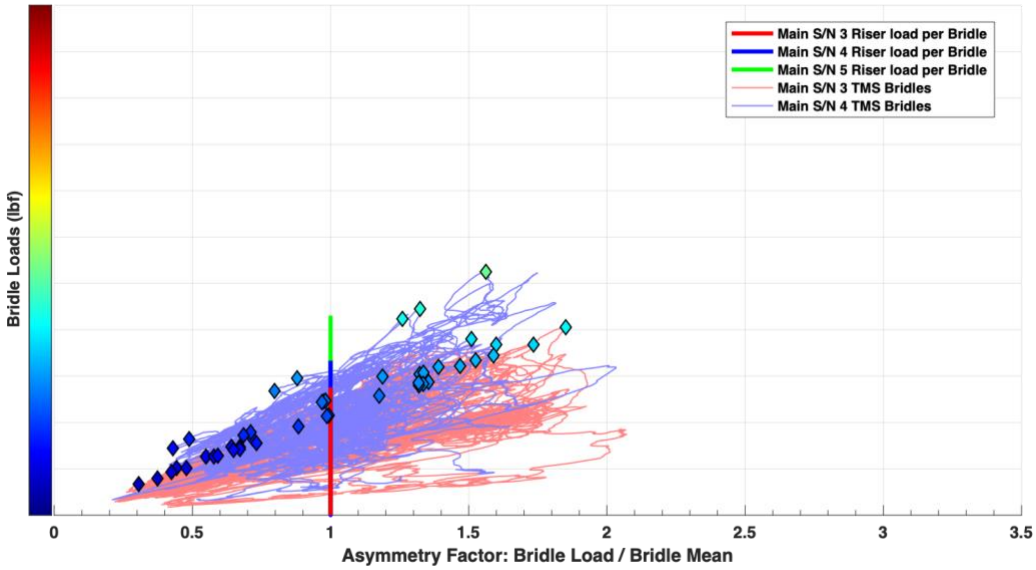

Figure 26. CDT-2-3 bridle line load vs asymmetry factor.

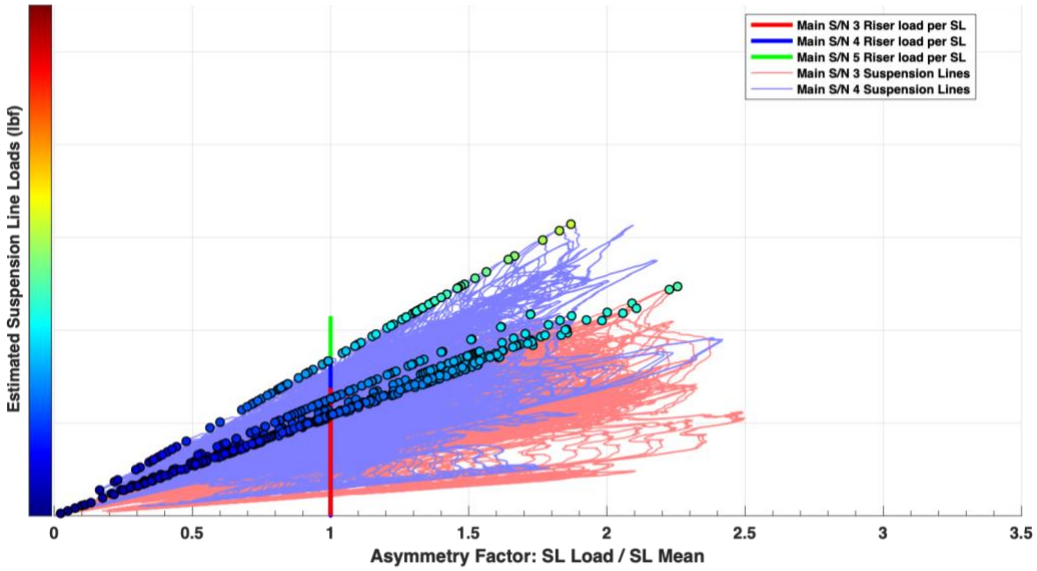

Figure 27. CDT-2-3 estimated suspension line load vs asymmetry factor.

Overlayed imagery and polar plots for the instrumented canopies on CDT-2-3 are shown at the times of peak load for all three stages in Figure 28, Figure 29, and Figure 30. The triangular formation of the cluster leads to more unique shapes and higher asymmetry than CDT-2-2, though with lower magnitude peak suspension line loads.

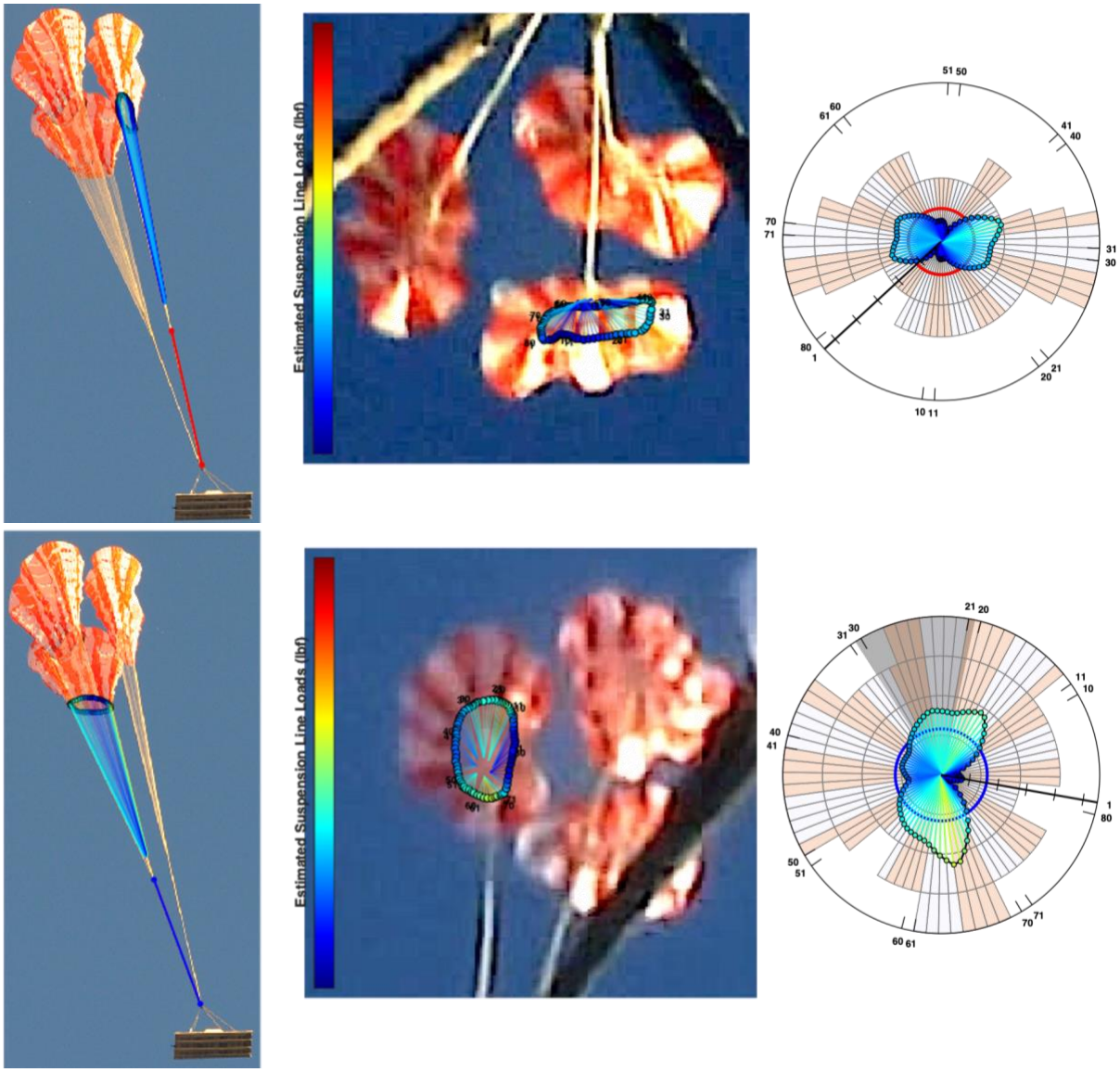

Figure 28. CDT-2-3 first stage estimated peak load distributions for Main S/N 3 (top) and Main S/N 4 (bottom).

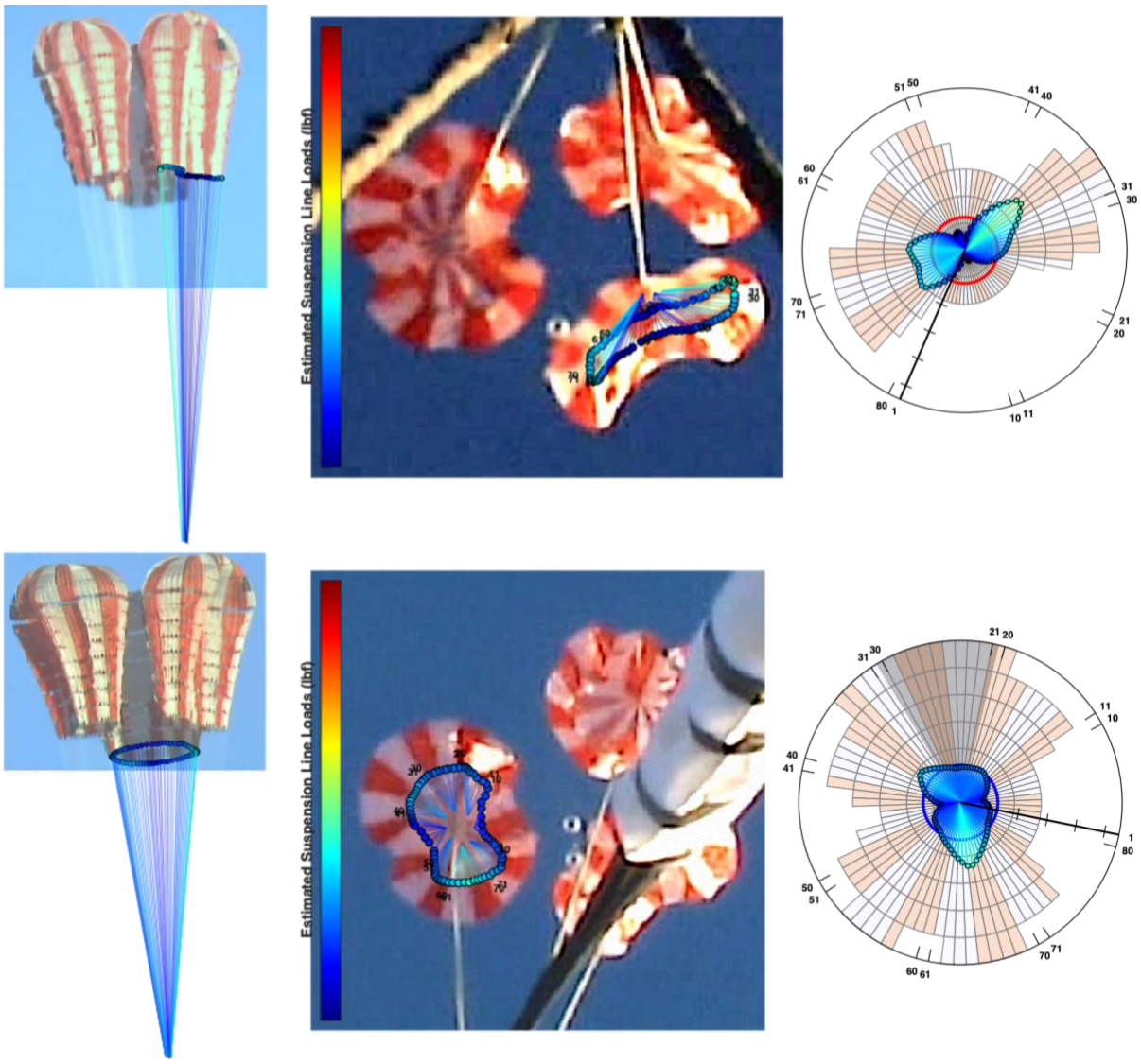

Figure 29. CDT-2-3 second stage estimated peak load distributions for Main S/N 3 (top) and Main S/N 4 (bottom).

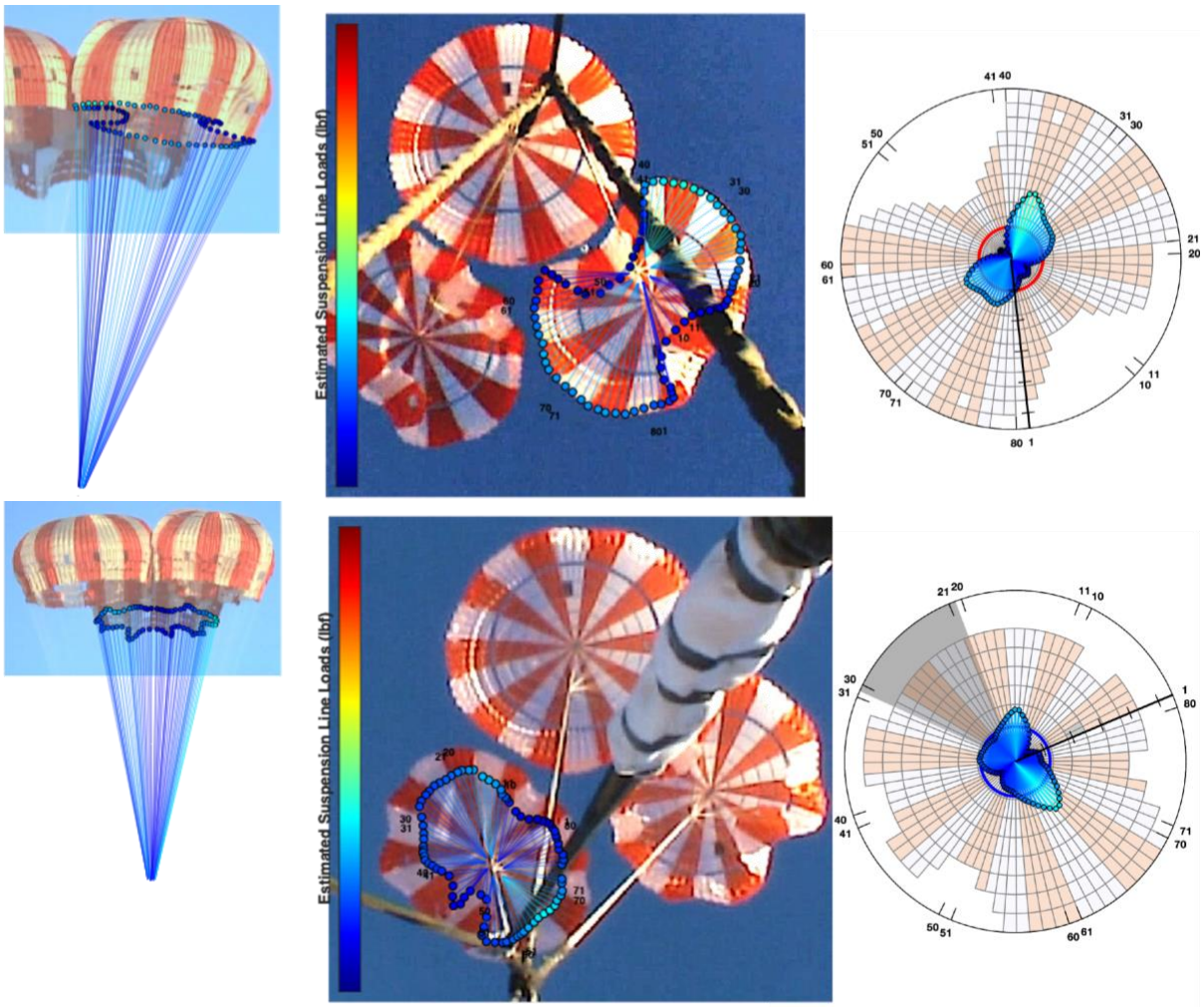

Figure 30. CDT-2-3 full open estimated peak load distributions for Main S/N 3 (top) and Main S/N 4 (bottom).

VI. Conclusion

Bridle-level asymmetry data collected on three early CPAS flights were revisited for finer analysis. Data from the flights were previously published, but some corrections were subsequently applied. An interpolation method was used to estimate the distribution of suspension line loads for computing a more accurate asymmetry factor. The asymmetry factors confirm that the standard value of 1.1 is not sufficient to describe main parachute inflation behavior. The data indicate that asymmetry factors around 1.5 at the bridle-level and around 2.0 at the suspension-line level should be expected at peak loads for main parachutes. Even higher asymmetry factors are associated with lower loads and would therefore not be relevant for design points. The further development of asymmetry instrumentation is highly recommended for all current and future human spaceflight parachute test programs.

Acknowledgments

The authors wish to thank Aaron B. Comis and John J. Rangel, both formerly of the NASA Commercial Crew Parachutes Team, for developing innovative techniques for parachute asymmetry analysis. Former CPAS analyst Christopher Russo assisted in mapping TMS data to canopy locations. NASA intern Kirk B. Putman helped develop the method for visualizing crown panel pressurization on behalf of the CCP.

References

[1] Morris, A. L., Olson, L., and Taylor, T., "Load Asymmetry Observed During Orion Main Parachute Inflation," *21st AIAA Aerodynamics Decelerator Systems Technology Conference*, Dublin, Ireland, May 2011, AIAA paper 2011-2611.

[2] Schmidt, J. R., McFadden, P. G., and Pritchett, V. E., "Parachute Asymmetry in Ares Development Tests," *21st AIAA Aerodynamics Decelerator Systems Technology Conference*, Dublin, Ireland, May 2011, AIAA paper 2011-2575.

[3] Knacke, T. W., "Parachute Recovery Systems Design Manual", Para Publishing, Santa Barbara, California, 1992.

[4] Morris, A. L., *et al*., "Summary of CPAS Gen II Testing Analysis Results," *21st AIAA Aerodynamics Decelerator Systems Technology Conference*, Dublin, Ireland, May 2011, AIAA paper 2011-2585.

[5] Romero, L. M., *et al*., "Summary of CPAS EDU Testing Analysis Results," *23rd AIAA Aerodynamic Decelerator Systems Technology Conference*, Daytona Beach, Florida, March 2015, AIAA paper 2015-2179.

[6]NovAtel, Inc., "IMU-HG," NovAtel, Inc. web site [online], 2009, URL: http://www.novatel.com/assets/Documents/Papers/HG1700_SPAN58.pdf [cited 18 August 2010].

[7]NovAtel, Inc., "SPAN-SE," NovAtel, Inc. web site [online], February 2010, URL: http://novatel.com/Documents/Papers/SPAN-SE.pdf [cited 23 March 2010].

[8] Ray, E. S. and Bretz, D. R., "Improved CPAS Photogrammetric Capabilities for Engineering Development Unit (EDU) Testing," *22nd AIAA Aerodynamic Decelerator Systems Technology Conference*, Daytona Beach, Florida, March 2013, AIAA paper 2013-1258.

[9] Moeller, J. H., "A Method of Load Prediction for Parachutes in Cluster," AIAA paper 1966-1507, and *Journal of Aircraft*, Vol. 4, No. 4, July-August 1967.

[10] Ray, E. S., "Reconstruction of Orion EDU Parachute Inflation Loads," *22nd AIAA Aerodynamic Decelerator Systems Technology Conference*, Daytona Beach, Florida, March 2013, AIAA paper 2013-1260.

[11] Ray, E. S., "Photographic Volume Estimation of CPAS Main Parachutes," *24th AIAA Aerodynamic Decelerator Systems Technology Conference*, Denver, Colorado, June 2017, AIAA paper 2017-3229.

[12] Janssen, S. A. and Ray, E. S., "Correlation of Canopy Distortion with Asymmetric Loading in Large Diameter Ringsail Parachutes," *26th AIAA Aerodynamic Decelerator Systems Technology Conference*, Toulouse, France, May 2022 (submitted for publication).

[13] Ray, E. S., "Reefing Line Tension in CPAS Main Parachute Clusters," *22nd AIAA Aerodynamic Decelerator Systems Technology Conference*, Daytona Beach, Florida, March 2013, AIAA paper 2013-1393.